

Structural Effects on Swelling of Thin Phosphorylcholine Polymer Films

Y. Tang and J. R. Lu*

Department of Physics, UMIST, PO Box 88, Manchester M60 1QD, UK

A. L. Lewis, T. A. Vick, and P. W. Stratford

Biocompatibles Ltd., Farnham Business Park, Farnham, Surrey GU9 8QL, UK

Received October 15, 2001

ABSTRACT: Spectroscopic ellipsometry (SE) has been used to monitor the time-dependent process of swelling of phosphorylcholine (PC) biocompatible polymer films of different initial dry film thicknesses. Factors including the extent of silyl cross-linker, ratio of hydrophilic and hydrophobic moieties, annealing temperature, and the composition of a set of polymer blends were assessed. The swelling of PC polymer films was found to follow a two-stage mechanism: a fast film expansion at the beginning of film immersion, followed by a much slow process controlled by the relaxation of polymer fragments. The two-stage swelling was well described by the coupled model developed by Berens and Hopfenberg, which assumed a simple superposition between the fast Fickian diffusion and the exponential decay accounting for the slow polymer fragment relaxation. Increase in annealing temperature to films incorporating 5 mol % silyl cross-linkers reduced the rate of swelling, which was attributed to the combined action of structure ordering and the strengthening of silyl cross-linking network. Increase in hydrophilic moieties substantially promoted the rate of swelling and their equilibrated water uptake, as expected. In the case of the blends from the two polymers with and without 5% silyl cross-linker, the swelling behavior was dominated by the cross-linked polymer.

Introduction

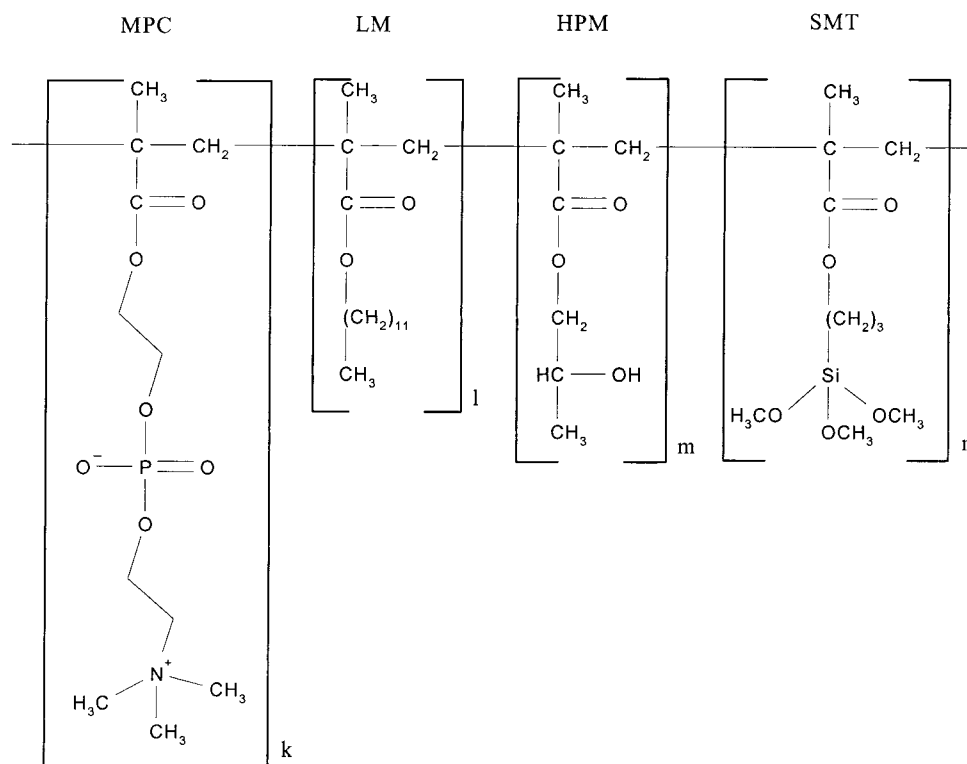
This paper describes the results on the swelling behavior of phosphorylcholine (PC) polymer films studied by spectroscopic ellipsometry (SE). The aim is to investigate the effects of silyl cross-linking, annealing conditions, and ratios of hydrophilic/hydrophobic components in the polymer on film swelling patterns. Although several studies have recently been done to characterize the biocompatible properties of PC polymers,^{1,2} little is understood about their swelling behavior and diffusion processes. Information relating to the dynamic swelling is highly relevant to the controlled drug delivery from these polymer films. Recently, we have shown that SE is well-suited for monitoring the time-dependent swelling of PC films.³ By simultaneously determining the two elliptical angles, ψ and Δ , we have been able to follow the variation of the extent of water penetrated into PC films with time. The earlier ellipsometric measurements on the cross-linkable PC polymer films (PC 100B) have revealed that these PC films can easily take some 60% water or more and that the extent of water uptake decreases with increasing annealing temperature. The current work aims to extend this study to the investigation of the effects of chemical composition and blending on the swelling of PC polymer films.

The dependence of swelling behavior on polymeric structure and environmental factors has been paid great attention by many researchers.^{4–13} The swelling phenomenon of polymers is usually classified as either Fickian diffusion, case II diffusion, or anomalous diffusion.^{14–17} These processes are separated by the relative rates of the Fickian diffusion of small penetrant molecules and the relaxation of polymer chains.^{18,19}

Several researchers have shown that adjusting the hydrophilic/hydrophobic ratios among polymeric networks can control the anomalous swelling behavior of polymer. In copolymer ethylene–vinyl alcohol (VA), both the observed equilibrium water sorption and the rate of water swelling were found to increase monotonically with VA content.²⁰ The experiments done by Peppas et al.^{13,21} showed that the water uptake was fast and that the copolymer film expanded with increasing hydrophilic component of P(HEMA-*co*-MMA) and P(HEMA-*co*-NVP) (*N*-vinyl-2-pyrrolidone). A similar trend was also observed in polymers consisting of poly(DL)-lactic acid and dextran segments²² and PHEMA/poly- ϵ -caprolactone and poly(DL)-lactide networks.²³ The effect of the extent of cross-linking on the dynamic swelling of polymer films has also been reported. Increase in the degree of cross-linking usually decreases the water uptake due to the reduced structural flexibility within the film.^{6,8} The dimension of polymer films has also been reported to affect the relative contributions of diffusion and relaxation, which in return alters the pattern of swelling.^{11,24–30} Because films used in biomedical coatings are typically of the order of submicrons, it is relevant to examine how the dry film thickness affects its swelling behavior.

From the perspective of biomedical coatings, it is of interest to explore how to control the kinetic swelling of PC polymer films through tailoring the ratio of hydrophilic and hydrophobic moieties in the polymer and the degree of cross-linking. This study together with the investigation of the effects of structural properties of these PC polymers on their surface biocompatibility and their subsequent performance in drug loading and release represents a set of essential assessments of biophysical properties before any further research is carried out toward the development of these PC polymer films for biomedical applications. In this paper we present the ellipsometry results on the characterization

* To whom correspondence should be addressed: e-mail j.lu@umist.ac.uk; Tel 44-161-2003926.

Scheme 1. Chemical Structure of PC Biocompatible Polymers; the Exact Molar Composition for Each Polymer Is Listed in Table 1**Table 1. Chemical Compositions of PC Polymer Samples**

polymer	composition (molar percentage)
PC100A	$K = 33, l = 67, m = n = 0$
PC100B	$K = 23, l = 47, m = 25, n = 5$
PC100C	$K = 47, l = 23, m = 25, n = 5$
PC82	PC100B:PC100A = 8:2
PC64	PC100B:PC100A = 6:4

of the dynamic swelling of PC films examined under different structural and environmental conditions. The main observation from this work is that the swelling was well described by a coupled two-stage model developed by Berens and Hopfenberg.³¹ The unusual relaxation process must be related to the structural rearrangement within the polymer network.

Experimental Section

Three PC polymers and two blends were used in this study. The chemical structure of the representative PC polymer (e.g., PC 100B) is shown in Scheme 1. The exact compositions for each of the PC polymers used are listed in Table 1. PC 100A has no silyl cross-linker while both PC 100B and PC 100C contain 5 mol % silyl cross-linking groups. All the polymers were copolymerized using part or all of the following monomers: 2-methacryloyloxyethylphosphorylcholine (MPC) (from Biocompatibles Ltd.), lauryl methacrylate (LM) (98%, Aldrich), 2-hydroxypropyl methacrylate (HPM) (96%, Aldrich), and trimethoxysilylpropyl methacrylate (TPM) (98%, Aldrich). The conditions for polymer synthesis and purification are described in ref 32. The polymerization was initialized using 1% AIBN (α, α' -azoisobutyronitrile), and the reactions were carried out at 62 °C in ethanol. PC 100A and PC 100B have a similar molar ratio of hydrophobic dodecyl groups to hydrophilic PC groups, but the former has no silyl cross-linker or 2-hydroxypropyl moiety. The molar ratio of dodecyl chains to PC groups was kept approximately at 2:1 for PC 100A and PC 100B, but this was around 1:2 for PC 100C. Blend polymers, PC 82 and PC 64, were formulated by dissolving the non-cross-linkable PC 100A and the cross-linkable PC 100B under different ratios

in the solvent of hexane and ethanol (1:1, volume ratio). The cross-linking reaction of PC 100B in the blends can still occur in the same manner as for pure PC 100B under annealing. However, the PC 100A chains could not participate in the cross-linking process and could only be constrained among the silyl network formed by PC 100B.

Silicon wafers were purchased from Compant Technology Ltd., UK, and were cleaned by immersing the wafers in dilute basic Decon solution (5%), followed by rinsing with Elgastat ultrapure (UHQ) water. Hexane and absolute ethanol from Aldrich (AR grades) were used as received.

Thin PC polymer films were prepared by dip-coating silicon wafers in PC polymer solutions using a specifically designed coating rig as described in ref 33. The mixture of hexane and ethanol in the volume ratio of 1:1 was used as solvent. For preparing films with thickness between 500 and 8000 Å, polymer solutions at different concentrations were made. To remove possible insoluble particles, the solutions were filtered through paper filters (Whatman) with pore diameters around 1 μm . Varying solution concentrations together with different motor lifting speeds helped to produce films with required thickness and persistent uniformity. The coated films were dried in air for at least 2 h at room temperature before they were annealed at 50, 100, and 150 °C for 3 h under vacuum. The samples were then left to cool to room temperature naturally and were then kept in a vacuum desiccator for subsequent characterization.

The thickness and optical constants of the polymer films coated on the silicon oxide substrate were measured with a variable angle spectroscopic ellipsometry (VASE, J. A. Woollam Co.). The dry film thicknesses were usually determined first at the air/solid interface with the film placed in the middle of the solid/liquid cell. The solid/liquid measurements were subsequently made after the solution was added.³ The measured ellipsometric data were analyzed to obtain the best-fit film thicknesses and refractive indices by WVASE software. The uniform layer model has been used to describe the distributions of water and polymer chains in the film, and the appropriateness of this assumption will be discussed later.

Because the films to be studied are very thin, water diffusion and film swelling occur almost entirely in the direction

perpendicular to the plane of the film. The instantaneous volume fraction of water, f_w , within the film at time t , is

$$f_w = \frac{V_t - V_0}{V_t} = \frac{\tau - \tau_0}{\tau} \quad (1)$$

where V_t and τ are the swollen film volume and film thickness at time t , and V_0 and t_0 are the dry film volume and film thickness, respectively. Following this linear relationship, the fraction of water uptake within the thin polymer film with respect to the final equilibrated amount can be calculated using the following equation:

$$\frac{M_t}{M_\infty} = \frac{f_w V_t}{f_{w,\infty} V_\infty} = \frac{\tau - \tau_0}{\tau_\infty - \tau_0} \quad (2)$$

where $V_t = A\tau$ and $V_\infty = A\tau_\infty$ (A is the surface area of the polymer film in contact with water and is assumed not to change with film swelling), M_t is the mass of water absorbed at any time t , M_∞ is the water amount at equilibrium, $f_{w,\infty}$ is the volume fraction of water at equilibrium, V_∞ is the equilibrium volume of swollen polymer film, and τ_∞ is the equilibrium thickness of polymer film.

Results

Swelling of PC 100A and PC 100B. The main structural difference between these two polymers is the inclusion of 5 mol % of silyl cross-linking groups in PC 100B. Their parallel ellipsometric measurements will enable us to examine the effect of silyl cross-linking groups on film swelling. We have shown in the previous study that films formed from cross-linkable PC 100B can approximately be described by uniform layer model.³ The same model has been used to test the PC 100A films which do not have the cross-linking groups. Lack of silyl cross-linking groups may lead to segregation and structural inhomogeneity along the surface normal direction. It is of interest to examine whether SE is sensitive to such structural details. Figure 1 shows the measured and fitted Ψ and Δ of a PC100A film in water, with the dry film thickness of 5900 Å. Two models were used to describe the water distribution in the PC 100A film (Figure 1a): a uniform layer with 60% of water throughout the film and a three-layer model consisting of a dry layer of 100 Å near the silicon oxide and a highly hydrated layer of 500 Å on the outer polymer surface. It can be seen from Figure 1b,c that the three-layer model gives a better fit than the uniform model. As the three-layer model fitting involved more parameters, this outcome would be rather well expected. It is however useful to note that both inner and outer layers in the three-layer model are relatively thin as compared to the middle layer, and their thickness increases tend to lead to the deterioration of the fits. More specifically, the middle layer in the three-layer model occupies 95% of the total material and contains 59% of water as compared with 60% from the uniform layer fitting. It can thus be said that the uniform layer model is still a good approximation to the description of structure of the non-cross-linking PC films. In the later discussion, the water volume fraction from the best uniform layer fitting will be used to denote the water content across the whole film.

Using the experimental procedures and fitting method established above, we have examined the swelling of a PC100A film annealed at 50 °C at the polymer/water interface, and the resultant Ψ and Δ are shown in Figure 2. The measurement of the dry film at the air/solid interface before film hydration gave the thickness

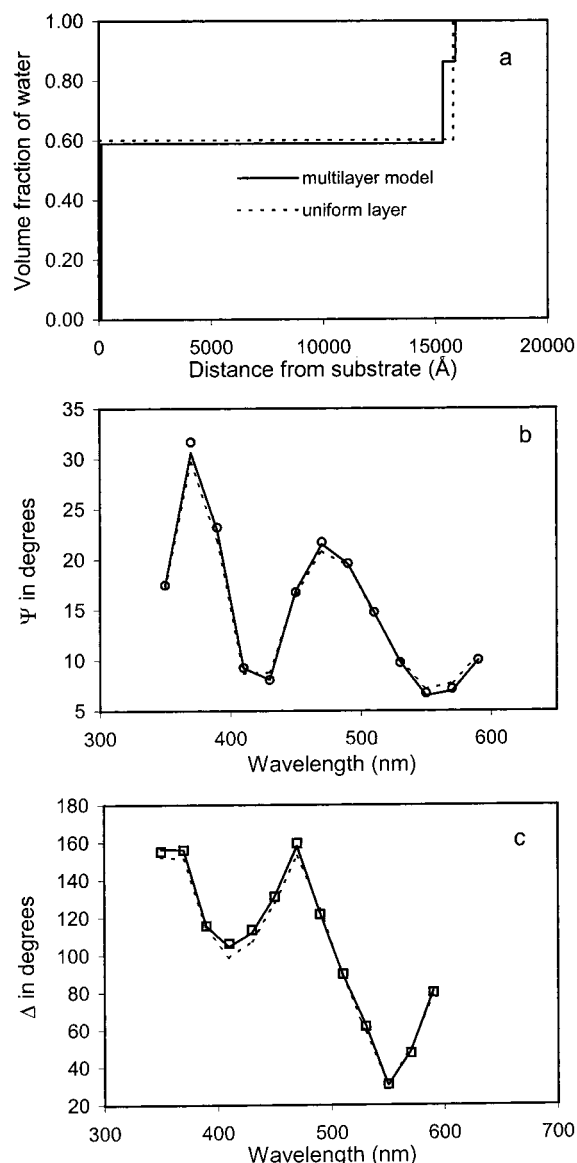


Figure 1. Single- and three-layer model fitting for a PC 100A film with an initial thickness of 5900 Å annealed at 50 °C, after 4 min immersed in water. (a) The solid line represents a three-layer model with an inner layer near SiO₂ of 100 Å and an outer water-rich layer near the water phase, 560 Å. The main hydrated PC 100A layer has a thickness of 15 200 Å and contains 59% water. The dotted line is a uniform layer model with a thickness of 15 800 Å and 60% water inside. (b) The measured Ψ data (circle) and fitted profiles. The solid line represents the three-layer model and the dotted line the uniform layer. (c) Measured Δ data (square) and the fits.

of 5900 Å with the refractive index around 1.55. From the parameters obtained from the dry film, the corresponding Ψ and Δ profiles against λ were calculated at the polymer/water interface at $t = 0$, and these are shown as dotted lines in Figure 2. The large gap between the calculated pair and the first set of the measured data indicates that a significant extent of swelling occurred within the first minute of film immersion in water. The subsequent changes in Ψ and Δ show that after the first several minutes the rate of film swelling slows down. This feature is similar to PC100B.³

The changes of thickness, refractive index, and water volume fraction of PC100A films under different initial thicknesses are shown in Figure 3 for films annealed at 50 °C and in Figure 4 for those annealed at 160 °C.

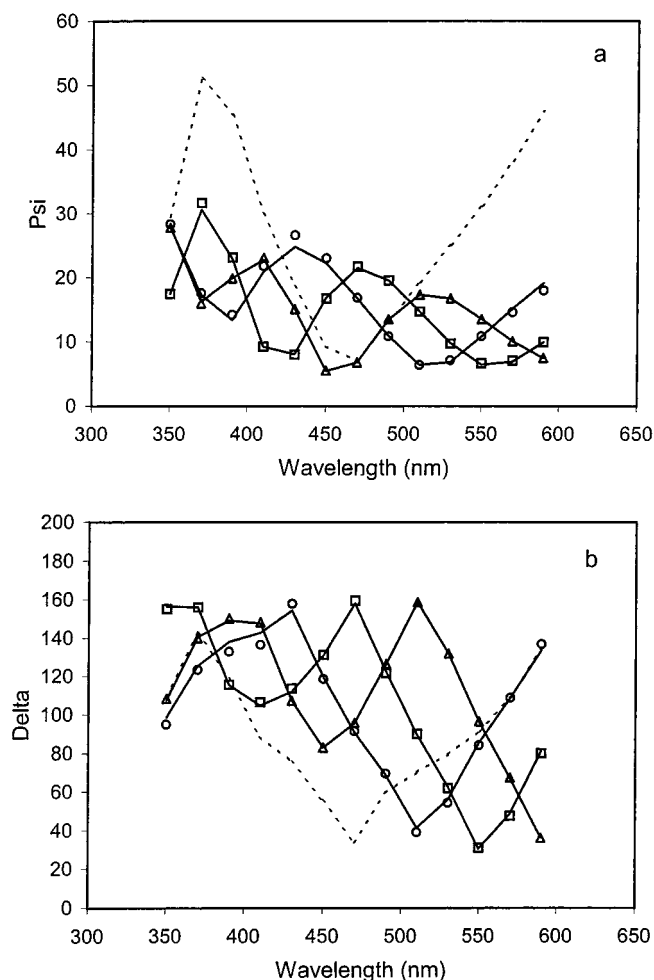


Figure 2. Ellipsometry scan to monitor the swelling of PC 100A film with an initial thickness of 5900 Å, annealed at 50 °C. (a) The change of Ψ data of PC 100A film swelling in water. The dotted line represents an assumed state of film in water at 0 min. Circles, squares, and triangles represent the measured Ψ at 1 min, 4 min, and 2 h of the film in water, respectively. The solid lines are the fitted results as determined by the three-layer model. (b) The change in Δ from PC 100A film swelling in water.

The degree of swelling, defined as τ_{∞}/τ_0 , for the two PC 100A films annealed at 50 °C is close to 3.30 after equilibration, indicating that swelling is not affected by dry film thickness. A similar trend is observed for the swelling of the two dry films annealed at 160 °C (Figure 4), but the degree of swelling is now only about 1.15, showing that as in the case of cross-linkable PC 100B films, annealing temperature is an important parameter affecting the extent of film expansion at the equilibrium state.

In addition to the difference in the equilibrated extent of water sorption, comparison of the profiles shown in Figures 3a and 4a shows different swelling dynamics. While the PC100A films annealed at 50 °C show a steady increase in swelling, those annealed at 160 °C show almost little change after the initial film expansion. The initial thickness jump for films annealed at 160 °C is likely to be caused by the presence of voids and cracks within the polymer films. The osmotic pressure generated by the penetrating water along the spaces in the polymer matrix makes the polymer film expand rapidly.

Figures 3b and 4b show the refractive index changes of PC 100A films under different annealing tempera-

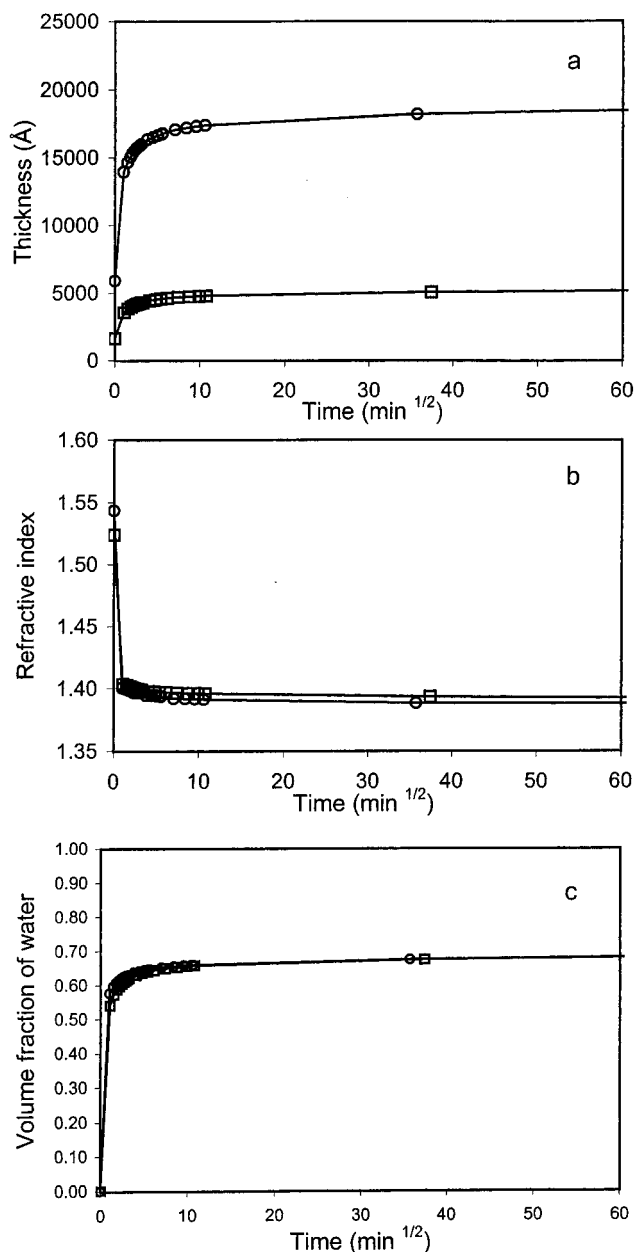


Figure 3. Film thickness (a), refractive index (b), and water volume fraction (c) of PC 100A films in water. The films were annealed at 50 °C. The circles represent the film with 5900 Å of initial thickness. The squares represent the film with an initial thickness 1640 Å.

tures. The refractive indices for the dry films of PC 100A polymers annealed at both temperatures are similar and are around 1.55. This is in contrast to the melting point of 120–130 °C for PC 100A detected by DSC. These results show that while thermal annealing above the melting point slows down the rate of swelling and the equilibrated amount of water uptake, structural changes within the film are not shown from refractive indices. The refractive indices for dry PC 100B films are around 1.48 and are thus lower than the values for PC 100A, and the difference is likely to be related to the chemical composition. While the ellipsometric results generally offer little indication about the structural features within the two types of PC polymer films, it is nevertheless interesting to note that the ellipsometric measurements showed that the PC100A films annealed at the higher temperature were not very transparent in the

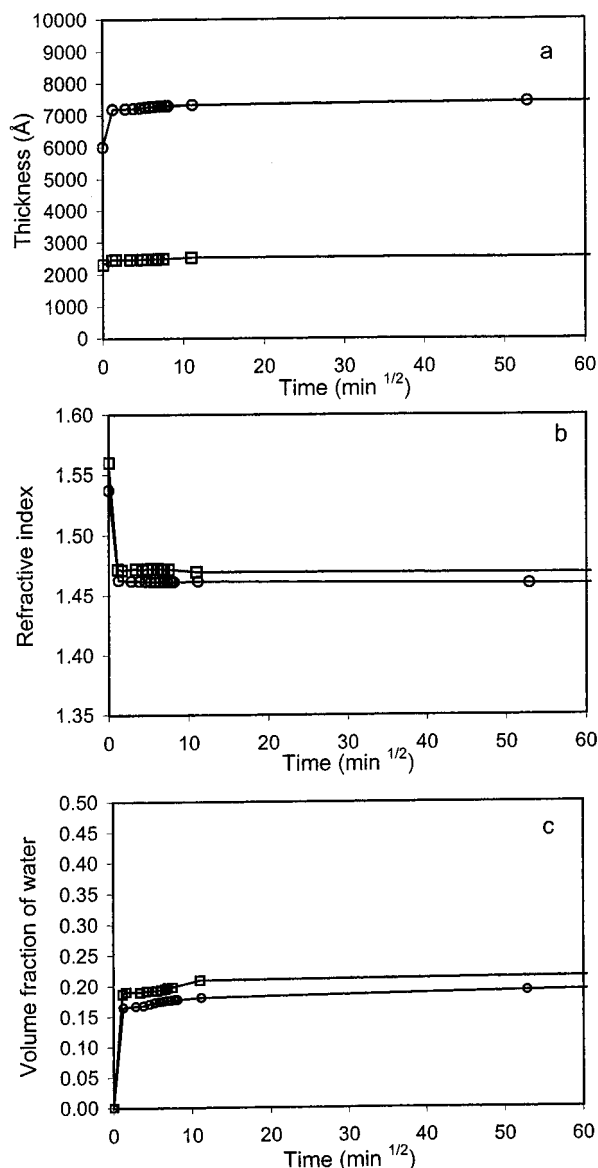


Figure 4. Film thickness (a), refractive index (b) (at $\lambda = 500$ nm), and water volume fraction (c) of PC 100A films in water. The films were annealed at 160 °C. The circles represent the film with an initial thickness 6000 Å. The squares represent the film with an initial thickness 2300 Å.

dry state. This could be seen as an indication of presence of some crystallites in the PC100A films. The lack of cross-linking groups in the PC100A polymers could favor the formation of crystalline structure. In contrast, the PC100B films under similar annealing treatment were transparent, thus suggesting no sign of crystallization.

Once water penetrated into the PC100A films, the refractive indices of PC100A decreased fairly rapidly to 1.40 for the samples annealed at 50 °C and to about 1.47 when annealed at 160 °C. If compared to the refractive index change of PC100B films, the respective refractive indices were found to be rather close between the two polymers in the course of swelling. Annealing temperature was again found to be the main factor affecting refractive index changes. The volume fraction of water in these polymer films can be obtained from the Maxwell–Garnett equation.³⁴ It can be seen from Figures 3c and 4c that the higher the annealing temperature, the lower the water content in polymer films.

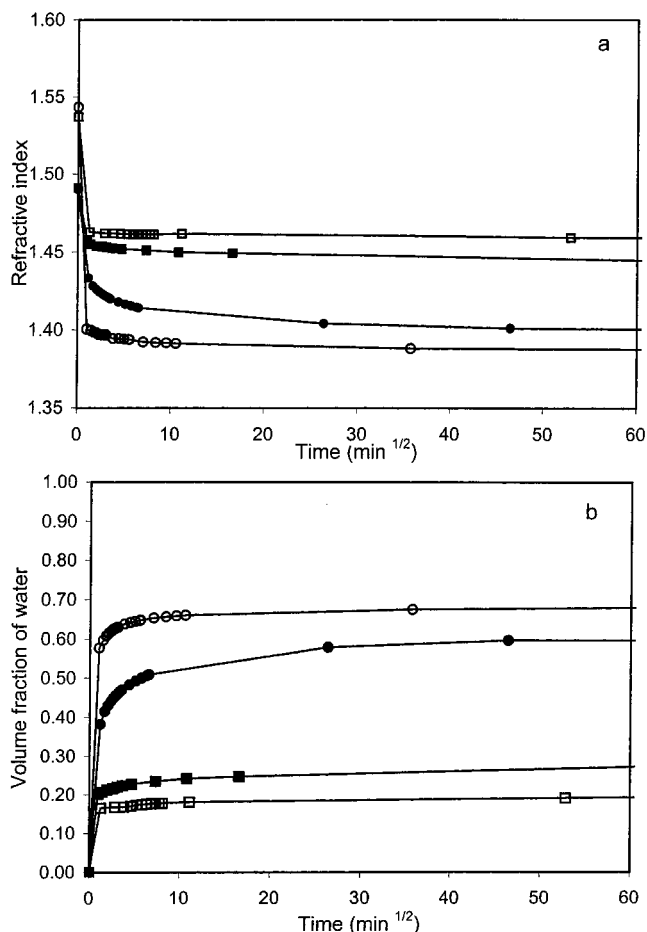


Figure 5. Comparison of PC 100A and PC 100B film swelling in water. The dry film thickness are 5900 Å for the PC 100A film annealed at 50 °C (open circle), 6000 Å for the PC 100A film annealed at 160 °C (open square), 5840 Å for the PC 100B film annealed at 50 °C (solid circle), and 5950 Å for the PC 100B film annealed at 150 °C (solid square). (a) Change of film refractive index with time. (b) Change of water volume fraction with time.

Table 2. Degree of Swelling (t_∞/t_0) of PC Polymer and Blend Films

polymer	annealing temperature	
	50 °C	150 °C
PC 100A	3.4 ± 0.1	1.1 ± 0.1 (160 °C)
PC 100B	2.5 ± 0.2	1.2 ± 0.2
PC 100C	8.3 ± 0.1	2.8 ± 0.2
PC 82	2.5 ± 0.3	1.5 ± 0.2
PC 64	2.7 ± 0.2	1.6 ± 0.2

In Figure 3c the two water volume fraction profiles are almost entirely overlapped, indicating that the water content in the films is insensitive to the dry film thickness when annealed at the low temperature. However, when annealed at the high temperature, the thinner film shows lower water content than that of the thicker one, as can be seen in Figure 4c. The difference is nevertheless under 5 vol % and is comparable to the experimental error.

In Figure 5 we compare the swelling behavior of PC polymer films with (PC 100B) and without (PC 100A) cross-linking groups. The values of t_∞/t_0 varying with annealing temperature are listed in Table 2. Two main interesting phenomena are observed. First, for the PC polymer films annealed at 50 °C, the water volume fraction of PC 100A polymer films is much greater than

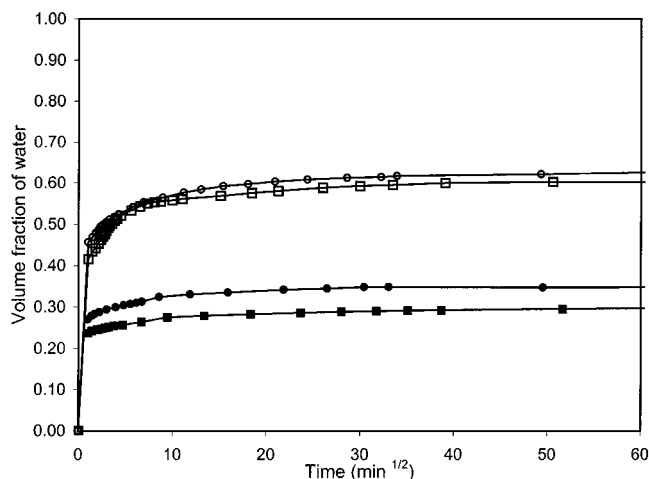


Figure 6. Change of water volume fraction of blend polymers with time. The dry film thicknesses are 3900 Å for the PC64 film annealed at 50 °C (open circle), 3900 Å for the PC82 film annealed at 50 °C (open square), 3850 Å for the PC64 film annealed at 150 °C (solid circle), and 3840 Å for the PC82 film annealed at 150 °C (solid square).

that of the cross-linkable PC100B films. This is reflected in the value of τ_{∞}/τ_0 of 3.4 for PC 100A, as compared to that of 2.50 for PC 100B. It may be that under such low annealing temperature only part of the cross-linking groups is cross-linked in PC 100B polymer films. The difference does however indicate that the silyl cross-linking network plays a role in the swelling, even at such a low annealing temperature. Since PC 100B contains some 25 mol % of 2-hydroxypropyl groups that strongly favor swelling, the reduced water volume fraction makes the constraining effect of silyl cross-linking even more pronounced. Second, for samples annealed at the high temperature, the degree of swelling is similar. In fact, the equilibrated water volume fraction in PC 100A films is slightly lower than that in the PC100B films. This result would tend to indicate that there is no obvious effect of cross-linking network in PC 100B on the swelling kinetics and that the substantial reduction in the rate of swelling and equilibrated water content result from the formation of a condensed structure. The inclusion of silyl-crossing network under this condition might only appear to render long-term chemical and mechanical stability. This is again not so when the strong swelling effect from some 25% 2-hydroxypropyl groups in PC 100B is taken into account. Thus, a comparable degree of swelling between the two polymer films is a convincing indication that the swelling of PC 100B films is controlled by both the condensed structure and silyl cross-linking network.

Swelling of Polymer Blends. The swelling behavior of blend polymers composed of PC 100A and PC 100B was also studied by ellipsometry. The molar ratios of PC 100B/PC 100A in two blend samples were 6/4 (PC 64) and 8/2 (PC 82), respectively. Figure 6 shows the thickness increase of blend polymer films, annealed at 50 and 150 °C, as a result of water intake. The swelling pattern of blend PC polymers largely follows the two individual polymers; i.e., the higher the annealing temperature, the slower the swelling rate and the lower the degree of swelling. While the main trend of swelling is similar at 50 °C, it can be seen from Figure 6 that PC 82 film clearly has lower water content than that of PC 64 film when annealed at 150 °C, suggesting that

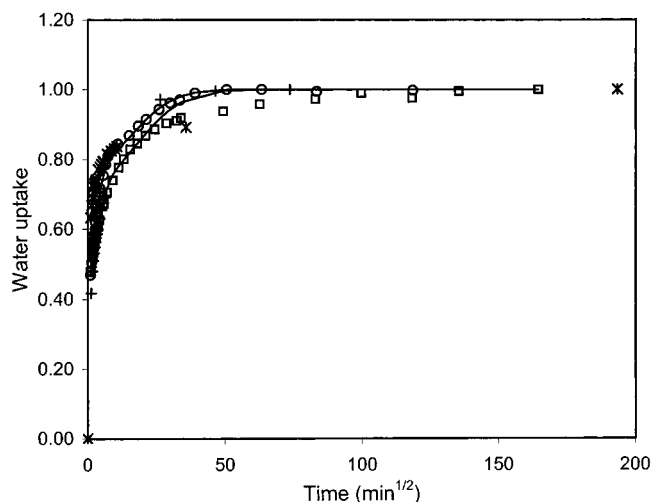


Figure 7. Water uptake of blend polymers: PC64 (square), PC82 (circle), PC 100A (cross), and PC 100B (plus). All samples were annealed at 50 °C. The continuous lines represent the best fits to PC64 and PC82.

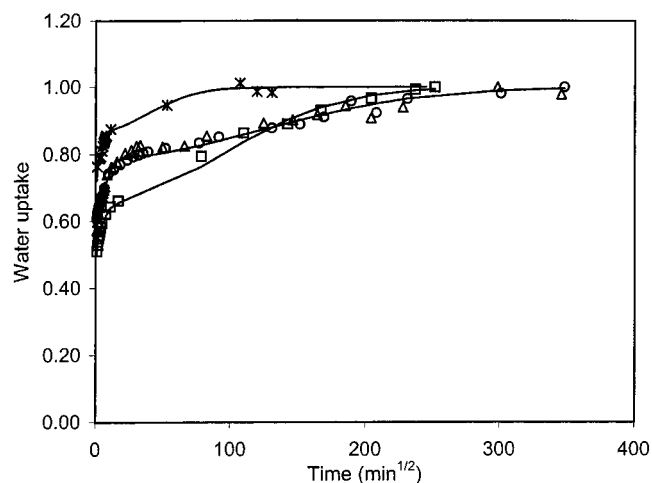


Figure 8. Water uptake of blend polymer: PC64 (triangle), PC82 (circle), PC 100A (cross), and PC 100B (square). The fitted lines overlap with their respective data points. All the samples were annealed at 150 °C, except for PC 100A which was annealed at 160 °C.

the extent of water uptake in the blends is dictated by the amount of cross-linkable PC 100B.

The relative changes in the swelling behavior between the blend polymers and the two individual polymers can be seen when their swelling profiles are compared. The results are plotted in terms of water uptake (M_t/M_{∞}) against time^{1/2} for different polymer films annealed at 50 °C (Figure 7) and those annealed at 150 °C (Figure 8). In this type of plot the differences in the variation of water uptake with time between four different polymers are rather small at the low annealing temperature, as can be seen in Figure 7. However, at the high annealing temperature substantial differences are now shown between the two individual polymers and the two blends. Note that this type of data plotting is complementary to the plotting of k_w vs time^{1/2} shown in Figure 5b. The main feature of Figure 7 is that Fickian diffusion is the dominating process, and the close resemblance between the four profiles indicates that, under this annealing condition, the four polymer films have comparable kinetic rates of swelling. However, as

will be discussed later, a mere Fickian process does not account for the entire swelling kinetics. Even under such a fast swelling process, polymer relaxation also contributes to the rate-controlling process.

As in the case of individual polymers, Figure 8 shows that the swelling of blend polymers annealed at 150 °C also displays a characteristic two-stage process. For all the polymers studied, the initial Fickian process is very fast, and it takes only a minute for the polymer films to take some 60% water. The subsequent slowing down is indicated by the deviation of the curves from the initial slope. The profiles from the two polymer blends sit in the middle of the two individual polymers. By comparing the water uptake of blend polymers with those of pure PC 100A and PC 100B, we find that it takes longer time for the blend polymers to equilibrate, implying that a longer time is needed for the polymer chains to relax in the blends.

Swelling of PC 100C. PC 100C has a molar ratio of 2:1 between the hydrophilic PC groups and hydrophobic dodecyl chains, as compared to a ratio of 1:2 in PC 100B. Their film swelling behavior under comparable conditions will enable us to assess the effect of hydrophilic/hydrophobic composition on the swelling kinetics and equilibrium water content. After measuring the thickness increase of PC 100C in water with time using the same conditions as those used for PC 100A, the degree of swelling for PC 100C films was found to be 8.39, 5.68, and 2.83 at the respective annealing temperatures of 50, 100, and 150 °C. These are compared with the corresponding values for PC100B of 2.48, 1.89, and 1.28. Since both PC 100C and PC 100B have the same amounts of silyl cross-linker (5%) and 2-hydroxypropyl groups (25%), these results show that increase in hydrophilic moiety increases the equilibrated water content. The swollen film of PC 100C annealed at 50 °C contained so much water that the film was easily broken by slightly shaking the silicon wafer.

The dynamic swelling process was also examined. As for other PC polymers, the swelling of PC 100C films also showed a two-stage sorption process. In comparison with PC100B, equilibration was reached more quickly in PC100C swelling. Silyl cross-linking induced by the high annealing temperature becomes more dominant in PC100C swelling as more hydrophilic segments are incorporated into the PC polymer.

The difference between the various polymers in swelling kinetics can also be compared by plotting M_t/M_∞ vs $\text{time}^{1/2}$, and the results are presented in Figure 9 for films annealed at 150 °C. PC 100A has no silyl cross-linking groups, and so it has the fastest rate of swelling. PC 100B has the slowest rate of swelling among the three polymers, given that it has some additional 25% 2-hydroxypropyl groups. The difference between PC 100A and PC 100B is largely attributed to the effect of silyl cross-linking. The time taken for the PC 100C polymer films to equilibrate is much shorter than that of the PC 100B polymer film, though both have the same degree of cross-linking and the same content of 2-hydroxypropyl groups. The faster swelling must arise from the higher content of hydrophilic PC moiety in the PC100C films. For clarity, the results for the two polymer blends are not shown in Figure 9, but it should be reminded that although the initial swelling largely overlaps between different polymers, the blends show the slowest relaxation process.

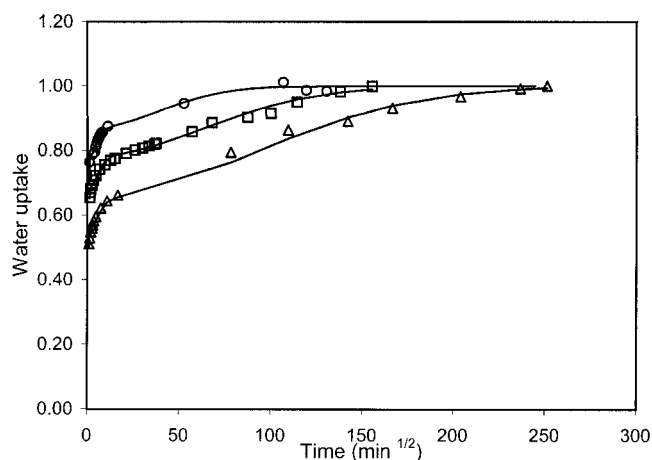


Figure 9. Comparison of water uptake of PC polymer films with different degrees of cross-linking and hydrophobic/hydrophilic ratios. The circles represent the PC 100A film annealed at 160 °C with an initial thickness of 6000 Å. The triangles represent the PC 100B film annealed at 150 °C with an initial thickness of 5900 Å. The squares represent the PC 100C film annealed at 150 °C with an initial thickness of 4500 Å. The solid lines are the fitted curves.

Discussion

Although diffusion of small molecules into polymer matrices has been extensively studied, little advance has been made in the understanding of swelling of thin polymer films. The new features of biocompatible PC polymer films arise from their thin film dimensions and unusual chemical compositions. The submicron dimensions of these films mean that they may not satisfy the boundary conditions defined for Fickian diffusion. Thus, most existing diffusion models may not be directly applicable to these PC films. In addition, almost all existing diffusion models have been developed using homogeneous polymer matrices such as PMMA and PS. This is in contrast to PC polymers containing distinct hydrophobic and hydrophilic moieties. Such diverse amphiphilicity within PC films is likely to lead to structural segregation to form percolated networks that introduce new features of swelling kinetics. Although SE has no sensitivity to structural details inside these films, the simultaneous fitting of Ψ and Δ to a uniform layer density distribution as found in this work suggests that any structuring within the layer must be isotropic along the surface normal direction.

The difference in the dynamic process of swelling between PC 100A and PC 100B may largely arise from the formation of silyl cross-linking network. We have explained in the previous work³ that there are three types of silyl cross-linking reactions upon annealing: cross-linking reactions between silane groups in the bulk of the film, those between the silane groups and hydroxy groups on the surface of silicon oxide, and those between the silane groups and organic hydroxy groups within the polymer films. The first two result in the formation of stable Si–O–Si bonds, and the last results in the formation of labile Si–O–C bonds. In all cases, increase in annealing temperature enhances the conversion process, providing films with strong chemical and mechanical stability. The increased strength of silyl network with annealing temperature imposes constraint on water uptake and film swelling kinetics. The rehydration of Si–O–C bonds within the polymer films is likely to be associated with the structural reorientations, which may cause the slow relaxation processes as

Table 3. Parameters Used in Simulating Profiles Shown in Figure 10

fitted parameters	curve 1 (PC100B (50 °C))	curve 2 (PC100B (150 °C))
initial thickness (Å)	6000	6000
fraction of Fickian diffusion	0.45	0.55
first relaxation rate constant (s ⁻¹)	8×10^{-4}	3×10^{-4}
second relaxation rate constant (s ⁻¹)	3.510^{-5}	1.0×10^{-6}
diffusion coeff (m ² s ⁻¹)	2.5×10^{-11}	7.0×10^{-12}

observed in Figure 9. Comparison between PC 100A and PC 100B shows that although the molar ratio of PC groups to dodecyl chains is similar and that PC 100B contains some 25% of hydroxyl groups, the overall swelling for PC 100B is slower, clearly indicating the constraining effect from the silyl cross-linking network. However, the intermediate swelling rate from PC 100C shows that, for the same amount of cross-linking, increase in PC groups increases the rate of swelling.

Although the relevant rate of dynamic swelling varies with the extent of silyl cross-linking and the ratio of hydrophilic and hydrophobic moieties, all the measured swelling profiles are characterized by the combined two-stage processes involving Fickian diffusion and polymer fragment relaxation. A semiempirical analytical equation that accounts for the coupled film swelling has been developed by Berens and Hopfenberg.³¹ In this model, the water sorption into glassy polymer is considered to be a linear superposition of Fickian diffusion and first-order relaxation. Crank¹⁸ has shown that for a plane film the analytical form of the Berens and Hopfenberg model can be expressed as

$$\frac{M_t}{M_\infty} = f_F \left[1 - \frac{8}{\pi^2} \sum_{n=0}^{\infty} \frac{1}{(2n+1)^2} \exp(-(2n+1)^2 k_F t) \right] + \sum f_{R,i} [1 - \exp(-k_{R,i} t)] \quad (3)$$

where

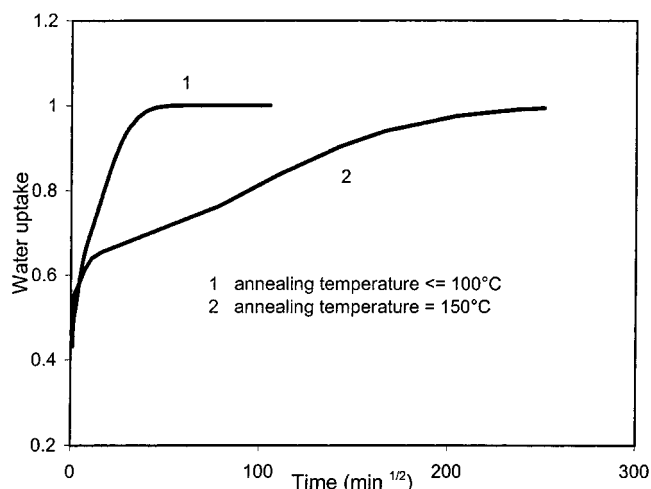
$$k_F = 4\pi^2 D / \tau_0^2 \quad (4)$$

$$f_F = 1 - \sum_i f_{R,i} \quad (5)$$

where f_F and $f_{R,i}$ are the fractions of contributions from the Fickian diffusion and relaxation processes and $k_{R,i}$ is the respective relaxation rate constant. Because of the thickness change of the polymer film during swelling, the diffusion coefficient D needs to be corrected to take into account of water volume fraction $f_{w,\infty}$ using the following equation

$$D = D^f (1 - f_{w,\infty})^2 \quad (6)$$

The parameters of k_F , $k_{R,i}$, f_F , $f_{R,i}$, and D , given in Tables 3 and 4, were obtained from direct fitting to the profiles of experimental M_t/M_∞ data vs time^{1/2}, and they

**Figure 10.** Simulated water uptake to demonstrate different patterns of PC polymer film swelling using eqs 3–5. Curve 1 represents a predominant Fickian diffusion process mimicking film swelling annealed below 100 °C. Curve 2 represents a slow two-stage swelling process mimicking the performance of PC films annealed at 150 °C.

were optimized by minimizing the least-squares residuals (χ^2). Two relaxation terms were found to be necessary to produce good fits to the experimental data profiles when eq 3 was used. The relaxation processes are size-independent, and the parameter k_F is inversely proportional to τ^2 according to eq 4. Thus, for the thin PC polymer films $k_F > k_{R,i}$.

The physical significance of the above equations can be comprehended when representative patterns of swelling are generated and compared. Figure 10 shows the two representative cases calculated from eqs 3–5, with the key physical parameters listed in Table 3. Curve 1 represents a typical Fickian-controlled fast swelling process with minor contribution from polymer relaxation. In contrast, curve 2 shows a more general case of slow swelling with main influence from polymer relaxation. The common feature of the two curves is that the first 60% water is absorbed into the films within seconds. The subsequent deviations from this initial step indicate the switch-over of the rate-controlling step from Fickian diffusion to polymer relaxation. This combined two-step swelling is qualitatively consistent with the feature observed for the PC polymer films.

With the schematic representations shown in Figure 10, it is tempting to apply eqs 3–5 to fit the measured data so that more consistent assessment can be made about the changes of swelling properties with respect to polymer structure and composition. The continuous lines through the measured profiles shown in Figures 7–9 were the best fits with the minima of χ^2 as the optimal fitting criterion. The parameters obtained from the fitting are listed in Table 4 for films annealed at 50 °C and in Table 5 for those annealed at 150 °C. It can be seen from Tables 4 and 5 that apart from the non-cross-linkable PC 100A the values for the fraction of Fickian diffusion (f_F) are all around 0.5 at the annealing

Table 4. Comparison of the Fitted Parameters for PC Polymer Films Annealed at 50 °C

parameters	PC100A	PC100B	PC100C	PC82	PC64
$\tau_0/\text{Å}$	5900 ± 75	5700 ± 20	5120 ± 15	3900 ± 20	3900 ± 20
f_F	0.63 ± 0.01	0.47 ± 0.01	0.53 ± 0.01	0.51 ± 0.02	0.51 ± 0.01
$f_{R,1}/\text{s}^{-1}$	$(1.03 \pm 0.14) \times 10^{-3}$	$(3.39 \pm 0.98) \times 10^{-4}$	$(1.58 \pm 0.17) \times 10^{-3}$	$(1.00 \pm 0.21) \times 10^{-3}$	$(6.34 \pm 0.45) \times 10^{-4}$
$f_{R,2}/\text{s}^{-1}$	$(5.45 \pm 1.00) \times 10^{-6}$	$(4.71 \pm 1.68) \times 10^{-5}$	$(4.36 \pm 0.20) \times 10^{-5}$	$(3.51 \pm 0.57) \times 10^{-5}$	$(2.86 \pm 0.16) \times 10^{-5}$
$D/\text{m}^2 \text{ s}^{-1}$	$(2.73 \pm 0.76) \times 10^{-11}$	$(1.05 \pm 0.84) \times 10^{-11}$	$(1.81 \pm 0.27) \times 10^{-10}$	$(7.43 \pm 4.03) \times 10^{-12}$	$(9.60 \pm 1.15) \times 10^{-12}$

Table 5. Comparison of the Fitted Parameters for PC Polymers Annealed at 150 °C

fitted parameters	PC100A (160 °C) ^a	PC100B	PC100C	PC82	PC64
$\tau_0/\text{\AA}$	6000 ± 50	5950 ± 20	4550 ± 10	3850 ± 20	3850 ± 10
f_F	0.77 ± 0.05	0.55 ± 0.01	0.68 ± 0.01	0.63 ± 0.01	0.61 ± 0.01
$f_{R,1}/\text{s}^{-1}$	$(4.37 \pm 7.68) \times 10^{-4}$	$(2.91 \pm 0.87) \times 10^{-4}$	$(3.10 \pm 0.36) \times 10^{-4}$	$(2.02 \pm 0.31) \times 10^{-4}$	$(2.40 \pm 0.43) \times 10^{-4}$
$f_{R,2}/\text{s}^{-1}$	$(5.78 \pm 6.69) \times 10^{-6}$	$(1.05 \pm 0.07) \times 10^{-6}$	$(2.12 \pm 0.15) \times 10^{-6}$	$(5.63 \pm 0.60) \times 10^{-7}$	$(4.91 \pm 1.02) \times 10^{-7}$
$D/\text{m}^2 \text{s}^{-1}$	$(5.84 \pm 7.61) \times 10^{-12}$	$(7.05 \pm 1.24) \times 10^{-12}$	$(1.09 \pm 0.12) \times 10^{-11}$	$(4.08 \pm 0.39) \times 10^{-12}$	$(4.17 \pm 0.87) \times 10^{-12}$

^a Annealed at 160 °C for 3.5 h.

temperature of 50 °C. These values increase to ca. 0.6 as the annealing temperature rises to 150 °C. More contribution from Fickian diffusion means less flexibility of chain movement within the polymer matrices due to either the intensified cross-linking or formation of condensed structure within the films. This trend is consistent with the overall decrease of both the first and second relaxation rate constants with annealing temperature. These observations are also in broad agreement with the decrease of the water diffusion coefficients with increasing annealing temperature. PC 100C contains most hydrophilic components and annealing caused most pronounced changes between these diffusion coefficients, a trend well predicted from the dominant effect of silyl cross-linking network. It is also added here that while the secondary order rate constants ($k_{R,2}$) remains virtually constant for PC 100A, $k_{R,2}$ drops by a factor of 20–60 for all other cross-linkable polymers when their films were annealed at the high temperature, again signifying the constraint of silyl cross-linking. It should however be reminded that although the extent of water swollen into the film was taken into account in the model, the dynamic variation of water in the course of swelling was not incorporated. In addition, the film structural expanding accompanying the water sorption process was not considered. These limitations means that the model may only predict the relative trends of variations and that the absolute values given in Tables 4 and 5 are most likely to be unreliable. This is especially so for the diffusion coefficients. Although the values of D appear to be comparable to those reported from other polymeric films for water diffusion within polymeric films,^{17,18} the physical significance relating to the absolute D values derived from these data analysis should be treated with caution.

Conclusions

The spectroscopic measurements described above have allowed us to investigate the dynamic process of PC film swelling with time. Three PC polymers and two polymer blends were used in this work. They together enable the effects of chemical composition of the PC polymers and the annealing conditions on film swelling and equilibrium water content to be examined. Since the PC films employed in biomedical coatings are mainly of the order of submicrons, the thicknesses of the films used in this work were largely fixed at ca. 6000 Å to mimic the situation. For films of this dimension, it was found that the structural features of the swollen films were not affected by the initial dry film thicknesses. At a given annealing temperature, both the equilibrium water content and the swelling kinetics are controlled by the presence of silyl cross-linkers, the ratio of hydrophobic dodecyl chains to the hydrophilic PC groups, and the inclusion of a hydrophilic 2-hydroxypropyl moiety. Increase in the hydrophilic components results in the increase in equilibrium water content and short-

ens the time required for reaching equilibration. The effect of silyl cross-linking is manifested via annealing temperature. Increase in annealing temperature not only intensifies silyl cross-linking but also helps to relax the tension imposed on polymer fragments and remove the voids and inhomogeneity in the polymer films. Thus, increasing annealing temperature reduces the equilibrium water content and prolongs the equilibration process.

The main finding of this work is that the swelling of all PC polymer films studied here follows a coupled two-stage process incorporating the fast Fickian diffusion and the slow polymer relaxation. This combined swelling phenomenon was well described by the Berens and Hopfenberg equation, though it is semiempirical.

Acknowledgment. Y.T. thanks Biocompatibles for a studentship and the British government for an ORS award. We thank EPSRC for support. We also thank Dr. J. Keddie at the University of Surrey for helpful discussions.

References and Notes

- (1) Hayward, J.; Chapman, D. *Biomaterials* **1984**, *5*, 135.
- (2) Murphy, E. F.; Lu, J. R.; Brewer, J.; Russell, J.; Penfold, J. *Langmuir* **1999**, *15*, 1313.
- (3) Tang, Y.; Lu, J. R.; Lewis, A. L.; Vick, T. A.; Stratford, P. W. *Macromolecules* **2001**, *34*, 8768.
- (4) Crank, J.; Park, G. S. *Diffusion in Polymers*; Academic Press: New York, 1968.
- (5) Han, H.; Gryte, C. C.; Ree, M. *Polymer* **1995**, *36*, 1663.
- (6) Kim, D.; Caruthers, J. M.; Peppas, N. A. *Macromolecules* **1993**, *26*, 1841.
- (7) Hill, D. J. T.; Moss, N. G.; Pomery, P. J.; Whittaker, A. K. *Polymer* **2000**, *41*, 1287.
- (8) Hariharan, D.; Peppas, N. A. *Polymer* **1996**, *37*, 149.
- (9) McNeill, M. E.; Graham, N. B. *J. Biomater. Sci., Polym. Ed.* **1993**, *5*, 111.
- (10) Durning, C. J.; Hassan, M. M.; Tong, H. M.; Lee, K. W. *Macromolecules* **1995**, *28*, 4234.
- (11) Ensore, D. J.; Hopfenberg, H. B.; Stannett, V. T. *Polymer* **1977**, *18*, 793.
- (12) Korsmeyer, R. W.; Peppas, N. A. *J. Membr. Sci.* **1981**, *9*, 211.
- (13) Korsmeyer, R. W.; Peppas, N. A. *J. Controlled Release* **1984**, *1*, 89.
- (14) Alfrey, A.; Gurnee, E. F.; Lloyd, W. G. *J. Polym. Sci.* **1966**, *C12*, 249.
- (15) Thomas, N. L.; Windle, A. H. *Polymer* **1982**, *23*, 529.
- (16) Frisch, H. L. *Polym. Eng. Sci.* **1980**, *20*, 12.
- (17) Bell, C. L.; Peppas, N. A. *Adv. Polym. Sci.* **1995**, *22*, 125.
- (18) Crank, J. *The Mathematics of Diffusion*, 2nd ed.; Clarendon Press: Oxford, 1975.
- (19) Hassan, M. M.; Durning, C. J. *J. Polym. Sci.* **1999**, *37*, 3159.
- (20) Hopfenberg, H. B.; Apicella, A.; Saleeby, D. E. *J. Membr. Sci.* **1981**, *8*, 273.
- (21) Brazel, C. S.; Peppas, N. A. *Polymer* **1999**, *40*, 3383.
- (22) Zhang, Y.; Won, C.-Y.; Chu, C.-C. *J. Polym. Sci., Part A* **1999**, *37*, 4554.
- (23) Barakat, I.; Dubois, Ph.; Grandfils, CH.; Jérôme, R. *J. Polym. Sci., Part A* **1999**, *37*, 2401.
- (24) Hopfenberg, H. B.; Frisch, H. L. *J. Polym. Sci., Part B* **1969**, *7*, 405.

- (25) Mathe, G.; Albersdörfer, A.; Neumaier, K. R.; Sackmann, E. *Langmuir* **1999**, *15*, 8726.
- (26) Frank, B.; Gast, A. P.; Russell, T. P.; Brown, H. R.; Hawker, C. *Macromolecules* **1996**, *29*, 6531.
- (27) Klitzing, R.; Möhwald, H. *Macromolecules* **1996**, *29*, 6901.
- (28) Durning, C. J.; Hassan, M. M.; Tong, H. M.; Lee, K. W. *Macromolecules* **1995**, *28*, 4234.
- (29) Sutandar, P.; Ahn, D. J.; Franses, E. I. *Macromolecules* **1994**, *27*, 7316.
- (30) Riggs, P. D.; Clough, A. S.; Jenneson, P. M.; Drew, D. W.; Braden, M.; Patel, M. P. *J. Controlled Release* **1999**, *61*, 165.
- (31) Berens, A. R.; Hopfenberg, H. B. *Polymer* **1978**, *19*, 489.
- (32) Lewis, A. L.; Cumming, Z. L.; Goreish, H. C.; Kirkwood, L. C.; Tolhurst, L. A.; Stratford, P. W. *Biomaterials* **2001**, *22*, 99.
- (33) Murphy, E. F.; Keddie, J.; Lu, J. R.; Brewer, J.; Russell, J. *Biomaterials* **1999**, *20*, 1501.
- (34) Born, M.; Wolf, E. *Principles of Optics*; University Press: Cambridge, 1997.

MA0117918